Evaluation of the Search and Rescue Leeway model into the Tyrrhenian sea: a new point of view

Antonia Di Maio[1], Mathew V. Martin[2], and Roberto Sorgente[3]

[1]Marine Technology Research Institute INSEAN, National Research Council of Italy, Rome, Italy
[2]Centre for Oceans, Rivers, Atmosphere and Land Sciences, Indian Institute of Technology Kharagpur, West Bengal, India
[3]Institute for Coastal Marine Environment IAMC, National Research Council of Italy, Oristano, Italy

Correspondence to: Antonia Di Maio (antonia.dimaio@cnr.it)

Abstract. The trajectories prediction of the floating objects above the sea surface represents an important task in the search and rescue (SAR) operations. In this paper we show how it can be possible to estimate the most probable search area by means of a stocastic model, schematizing appropriately the shape of the object and evaluating the forces acting on it. The LEEWAY model, a Montecarlo-based ensemble trajectory model, has been used: here both the statistical law to calculate the $leeway$ and an $almost$ deterministic law inspired by the boundary layer theory have been considered. The model is nested with the sub-regional hydrodynamic model TSCRM (Tyrrhenian Sicily Channel Regional Model) developed in the framework of PON-TESSA (National Operative Programs-TEchnology for the Situational Sea Awareness) project. The main objective of the work is to validate the new approach of $leeway$ calculation relying on a real event of Person in Water (PIW), occurred in the Tyrrhenian Sea in July 2013 . The results show that by assimilating a human body to a cylinder and estimating both the transition from laminar to turbulent boundary layer and the drag coefficients, it can be possible to solve a forces balance equation which allows to estimate the search area with good approximation. This new point of view leads to the possibility to check the same approach also on other different categories of targets, so as to overcome in the future the limitations associated with calculation of $leeway$ by means of the standard statistical law.

Keywords. LEEWAY Model, $leeway$, Person In Water, Search and Rescue

1 Introduction

Meteocean and environmental forecast are being increasingly used in operational decision making in the sea for demographic, geographic and strategic applications. Safety and assets at sea are a shared objective of many countries: having an efficient ocean forecast system is essential to improve prediction of sea and to provide useful environmental ocean information so as to increase the effectiveness of search operations (Breivik et al., 2013). In the event of accident, timely Search and Rescue (SAR) intervention is helpful in significantly lowering the loss of life and also to contain the damage. A considerable amount of resources is currently invested in maintaining SAR capabilities by major maritime nations. However, on many occasions, the available SAR capabilities prove to be inadequate to provide timely assistance in distress scenarios. Nevertheless, the effectiveness of the available SAR capabilities can be increased if we exploit the high-quality environmental forecast data for

SAR planning. An example of operational ocean forecasting and services coupled with Search and Rescue (SAR) activities are represented by GODAE BLUElink operational ocean prediction system (Brassington et al., 2007), used by the Australian Maritime Safety Authority. A list of global and regional operational ocean forecasting systems, supported by the Global Ocean Data Assimilation Experiments - GODAE (Bell et al., 2009), can be found in Davidson et al. (2009), while a recently review of the evolution of the global and regional forecasting system from GODAE into GODAE OceanView (Bell et al., 2015) is described in Tonani et al. (2015). These systems are based on ocean general circulation models (OGCM) and data assimilation techniques that are able to correct the model with information inferred from different types of observations, acquired by various sensors and platforms.

In the coastal areas, the high-frequency radars are crucial to acquire the surface two-dimensional current data (Barrick et al. (1977); Barrick et al. (2012); Cianelli et al. (2015); Paduan and Rosenfeld (1996)). Maps acquired by a coastal HF radar have been used both to obtain backtracked trajectories of floating object (Abascal et al. (2012); Abascal et al. (2009b); Berta et al. (2014)) and for SAR applications (Ullman et al. (2006); Ullman et al. (2003)). Some european countries performed an important effort toward the implementation of national HF radar networks (Quentin et al., 2013); (Carrara et al., 2014), but at present just one unified HF coastal radar network is started in the Mediterranean Sea. It is the Tracking Oil Spill and Coastal Awareness (TOSCA) network, covering the Aegean, Adriatic, Tyrrhenian, Ligurian and Balearic Seas; it started as support for decision-making process relative to marine accidents concerning oil spill pollution and search and rescue (SAR) operations (Bellomo et al., 2015). TOSCA network currently covers sensitive and environmentally relevant areas, affected by intense ship traffic and/or the presence of oil pipelines; nevertheless it is only the first step towards the building of an integrated HF radar system in the Mediterranean regional alliance and its coverage is relatively small yet, so it is not always involved in the ocean forecasting systems nor in the connecting application such as the SAR planning.

The first step in marine search planning is to determine the most probable area containing the searched object and that is even more important if the target is person in water (PIW). The definition of the probable search area is essentially linked to the quantification of some unknowns, such as the Last Known Position (LKP) and typology, shape and dimensions of the objects. Moreover, a PIW or object without propulsion is also subject to drift from ocean currents, wave action and direct wind action (Davidson et al., 2009). Hence, an effective SAR planning requires accurate environmental forecasting, especially regarding surface currents, temperature and surface winds for short range time-scale. Today, such information can be provided in near real time (NRT) from global and regional operational oceanography systems following from the successful implementation of the Global Ocean Observing System (GOOS).

In the Mediterranean Sea, operational forecast starting from the year 2000 are provided by the Mediterranean Forecasting System - MFS (Tonani et al., 2008). The MFS uses a horizontal grid of resolution of 1/16° and provides detailed forecast at a regional scale for the whole Mediterranean basin. The fundamental part of the system is the assimilation scheme for the blending of the observations into the model in order to provide the most accurate description of the past and the best initial condition for the forecast fields at large scale (Oddo et al., 2009).

In many cases, SAR activities may also require fields of interest on a high spatial resolution. Sub-regional forecast systems that can resolve small-scale processes as well as fronts characteristics of the study area are necessary. A numerical technique widely

used in operational oceanography to increase the horizontal resolution is the downscaling procedure, which permits to adapt the large scale features to the coastal areas by means of model domains cascade embedded (Pinardi et al., 2003). This has been achieved through implementation of a nested high resolution ocean model for the central Mediterranean basin developed in the framework of the project Development of TEchnology for Situational Sea Awareness (TESSA). This hydrodynamic model, named Tyrrhenian and Sicily Channel sub-Regional Model (TSCRM), is based on POM (Blumberg and Mellor, 1987) and has a horizontal resolution of 1/48°, equal to three time MFS.

TESSA project is supported by PON "Ricerca e Competivita' 2007-2013", which is a National Operational Programme of the Ministry for Education, University and Research of Italy. The general aim is to improve the products and services of the operational oceanography in Southern Italy and to integrate them with technological platforms. The latter are set up to disseminate information for the Situational Sea Awareness (SSA) also in support to the SAR activities at sea. In Italy these activities are performed by the Coast Guard, within the competence of the Ministry of Infrastructures and Transport of Italy.

In this paper we present some numerical results about the prediction of PIW trajectories in the central Tyrrhenian Sea. We use two different approaches for the $leeway$ calculation: the first approach is standard and it consists in the $leeway$ calculation by means of the statistical parameters tabled by Allen and Plourde (1999). The second one is a variant of the first approach: it consists in the $leeway$ calculation by means of the forces balance equation based on modifications of the target boundary layer. The main of this work is to validate the latter approach. We hope that in the near future the new method will permit to define a practical formula of $leeway$ calculation helpful not only in similar PIW cases but also in other targest cathegories.

The new approach is embedded in the LEEWAY model, a drift model based on a stochastic approach (Breivik and Allen, 2008), combined with environmental forecast data from TSCRM and European Centre for Medium Whether Forecast (ECMWF). The ensuing sections of the paper are organized as follows: section 2 describes the models used and the numerical experiments; an analysis of the model results is presented in section 3 together with possible future extensions. A summary and concluding remarks are given in section 4.

2 Material and Methods

In this section we describe our drift forecast operational numerical model developed to predict the trajectories of floating objects (SubSection 2.1), the characteristics of the LEEWAY model including also our variation about the calculation of the $leeway$ (SubSection 2.2) and the different experiments (SubSection 2.3) based on Person In Water (PIW).

2.1 Ocean Model

The current forecasting model used in this work is the Tyrrhenian and SiCily strait sub-Regional Model (TSCRM), an operational sub-regional, nested ocean model implemented into the central Mediterranean Sea during the framework of the project TESSA. TSCRM is a free surface three-dimensional primitive equation finite difference hydrodynamic model, based on the Princeton Ocean Model - POM (Blumberg and Mellor, 1987). It solves the equations of continuity, motion, conservation of temperature, salinity, the model assumes that the fluid is hydrostatic and the Boussinesq approximation is valid. The density is

calculated by adaptation of the UNESCO equation of state revised by Mellor (1991); the horizontal viscosity and vertical mixing coefficients are computed respectively using the Smagorinsky approach (Smagorinsky, 1993) and the Mellor and Yamada (1982) turbulence closure scheme. It is an extension of the Sicily Strait sub-Regional Model implemented by Sorgente et al. (2011), and successively made operational by Fazioli et al. (2015) and embedded into the regional model of the MFS (Tonani et al., 2008) through the downscaling procedure (Sorgente et al., 2003). This modelling technique, widely used tp produce numerical weather prediction (Koch and McQueen, 1987), allows to downscale the model results from the regional scale to the sub-regional scale by transmitting values of temperature, salinity and velocity (three-dimensional fields daily mean) at the interconnecting boundaries from the coarse resolution grid to the fine resolution. That permits a more detailed description of the circulation in those areas where the regional model cannot resolve the small mesoscale features. By means of the downscaling technique, TSCRM receives informations at lateral open boundaries by an off line, one-way asynchronous nesting technique (Zavatarelli et al., 2002), coupling to the regional model with which it is embedded. Surface momentum and buoyancy fluxes are interactively calculated through standard bulk formulae. The latter use Sea Surface Temperature as predicted by the model, and 6-h (00:00, 06:00, 12:00, 18:00 UTC) and 0.25° atmospheric variables provided by the European Centre for Medium Range Weather Forecast operational analyses (Sorgente et al., 2011). TSCRM produces 1-h and 1/48° fields that are used with the 6-h and 0.25° wind velocity fields to force the lagrangian model LEEWAY.

2.2 LEEWAY model

The drift of a floating object above the sea surface is the result of the balance between the hydrodynamic and aerodynamic forces. This balance induces the object to move with a certain angle relative to downwind direction (Richardson, 1997; Breivik and Allen, 2008), therefore it is foundamental to take into account the $leeway$ to estimate the trajectories of drifting objects with good approximation.

The term $leeway$ refers to object's motion induced by the atmospheric wind (10 m reference height) and waves relative to ambient current (between 0.3 and 1.0 m depth). This definition standardized the reference levels for the measurements of $leeway$ for SAR objects and provides a practical way to utilize current and wind vectors from numerical models (Allen, 2005). The empirical relation between $leeway$ and wind speed is given by empirical coefficients (linear regression coefficients and their standard deviations) for a total of 63 different targets classes, tabled as a result of field campaigns performed by the U.S. Coast Guard (Allen and Plourde, 1999). These coefficients give an estimate of the relation between the wind speed and the $leeway$ velocity vector, converted into following components: a downwind component and positive (right of the wind) and negative (left of the wind) crosswind $leeway$ components (Allen, 2005); they are explicited in the following equations:

$$\boldsymbol{L_d} = (a_d + \epsilon_d)\boldsymbol{W_{10m}} + b_d + \epsilon_d \tag{1}$$

$$\boldsymbol{L_c^+} = (a_c^+ + \epsilon_c)\boldsymbol{W_{10m}} + b_c^+ + \epsilon_c \tag{2a}$$

$$\boldsymbol{L_c^-} = (a_c^- + \epsilon_c)\boldsymbol{W_{10m}} + b_c^- + \epsilon_c \tag{2b}$$

The wind velocity vector $\mathbf{W}_{10m}$ is the wind speed measured at $10m$ reference height, or simulated by a weather forecast model. The term L_d of equation (1) represents the downwind $leeway$ component (DWL), while the terms L_c of equation (2a) and (2b) are the crossway $leeway$ components (CWL), that are the divergence of the SAR object from the downwind direction. The parameter a is denoted the $leeway$ rate ($leeway$ to wind ratio), b is the regression intercept at zero wind and ϵ the regression residual (Breivik et al., 2012). The determination of the $leeway$, or rather the relation between the wind speed and the $leeway$ speed and divergence angle, gives a measure of how much the wind directly pushes on a object floating at the sea.

It is necessary to assume that the empirical coefficients of linear regression of the equations 1 and (2a) and (2b) also include the contribution of the Stokes drift (Breivik and Allen, 2008). Following this we assume that $leeway$ can be only expressed as a function of the wind and we use a practical definition of $leeway$ which doesn't tell the wind and wave influence apart. This approximation can be also extend to other small objects and to most sea states, according to Breivik et al. (2012).

By estimating the DWL and CWL $leeway$ linear regression coefficients, it is possible to recreate the expected drift of an object by means of modelled or measured data concerning the wind and sea current. As the LEEWAY model uses empirical formulae and imperfect approximation to the hydrodynamic laws, a Monte Carlo technique works to generate an ensemble through random perturbations; the ensemble allows to take into account the uncertainties about the forcings (wind and current), $leeway$ drift properties (draught, length and beam), and the Last Know Position (LKP) of the search object. The trajectory is then obtained by estimating at each time step the corresponding probability density function of containment of the object, and its envelope is the estimation of the search area (Davidson et al., 2009).

An exhaustive description of the stochastic approach used into the LEEWAY suite is given by Hackett et al. (2006).

In this work we present a variation about the calculation of the $leeway$ replacing the linear regression equation described by equations (1), (2a) and (2b) with an $almost$ (due to uncertainties in forcing fields) deterministic law which is the balance of the aerodynamic and hydrodynamic forces acting on the target, evaluating the modification of its boundary layer. The target is supposed approximately symmetrical, therefore the lift can be neglected; we suppose that such target is tracked by the surface current under the hypothesis of steady motion:

$$\boldsymbol{F_P} + \boldsymbol{F_A} + \boldsymbol{F_{ADw}} + \boldsymbol{F_{ADa}} = \mathbf{0} \tag{3}$$

where $\boldsymbol{F_P}$ is the weight force, $\boldsymbol{F_A}$ is the Archimedes force, $\boldsymbol{F_{ADw}}$ is the active drag force in water and $\boldsymbol{F_{ADa}}$ is the active drag force in air. The first two forces give the emerged/submerged ratio, whereas the last two forces are responsible for the transport in the horizontal plane.

The equation (3) is solved on vertical and horizontal planes. In the vertical plane, the equation is the balance between weight force and Archimede reaction and its solution means just using the reduced mass of the target.

On the horizontal plane we solve the equation distinguishing between laminar and turbulent boundary layer. The resistence to the motion for a laminar boundary layer is given only by the viscosity friction and so we solve the Stokes law:

$$\mu_w \cdot R_W \cdot (\boldsymbol{u_c} - \boldsymbol{u_B}) + \mu_A \cdot R_A \cdot (\boldsymbol{w} - \boldsymbol{u_B}) = 0 \tag{4}$$

where μ_w and μ_A are the water and air viscosity, respectively; R_W and R_A is the submerged and emerged radius; $\boldsymbol{u_c}$ and $\boldsymbol{w}$ are the current and wind velocity, while $\boldsymbol{u_B}$ is the object velocity.

If the boundary layer is turbulent the resistence to the motion is given by the balance of the kinetic energy exchange between the moving body and the fluids:

$$\frac{1}{2} \cdot C_{D_W} \cdot \rho_w \cdot S_S \cdot (\boldsymbol{u_c} - \boldsymbol{u_B})^2 + \frac{1}{2} \cdot C_{D_A} \cdot \rho_A \cdot S_E (\boldsymbol{w} - \boldsymbol{u_B})^2 = 0 \tag{5}$$

where S_S and S_E are the submerged and emerged area and C_{D_W} and C_{D_A} are the corresponding drag coefficients.

Finally we estimate the Probability of Containment (POC) overlapping a spatial grid on the geographycal one; we set arbitrarly each grid box to 0.06x0.06° and we calculate the particles percentage for each grid box, assigning a color bar from blue to red to distinguish the corresponding POC values from a minimum to a maximum value. The probability cumulative value is calculated summing the values of highest probability of the individual cells then it could correspond to cells not geographycally consecutive. A final diary is written to storage the vertices of the cells of high probability.

2.3 Numerical Experiments

In this work the LEEWAY model is used to reproduce a real event occurred in the western Tyrrhenian Sea, along the coast of Sardinia: on July 11^{th} 2013 a man was seen for the last time at UTC 08:30pm (Start point) approximately on board of a ferry that was on duty from Cagliari (Sardinia Island) to Civitavecchia (Italy) and only shortly before midnight of the 12^{th} July 2013 (End point) the alert was given. His body was retrieved at UTC 10:30am of 12^{th} July 2013 in a point of known coordinate (Tab. 1).

The LKP is a critical step, as the accuracy of this information is decisive for the outcome of the search. In this task, we represent it as a line between start and end points (Tab. 1) recorded from the Automatic Information System data provided by General Headquarters of the Italian Coast Guard (Fig. 1).

Numerical simulations of PIW trajectories are run using two different methodologies. The first one consists in the $leeway$ calculation by means of the equations described in (1), (2a) and (2b), while in the second one the $almost$ deterministic laws described by equations (4) and (5) are used.

In both the methodologies we rely on the conclusions of Breivik and Allen (2008) about the forcings perturbation, therefore they are considered of secondary importance especially in our stable and relatively homogeneous conditions. We use the mean standard deviation of the current and wind components, calculated on the spatial grid and on the period of the simulation (43 hours): the estimate is 0.07 $m \cdot s^{-1}$ on current east component and 0.1 $m \cdot s^{-1}$ on the north one, while it is 2.68 $m \cdot s^{-1}$ on wind east component and 2.93 $m \cdot s^{-1}$ on the north one.

We perform three different sets of experiments seeding a total of 1000 particles in 8 time steps from start to end point of Last

Know Position and subsequently estimating the smallest distance between the mass center of each subset of particles and the retrieval point.

The first set of experiments is a check about the target tabled configurations (sitting, vertical, horizontal/survival, horizontal/deceased and $unknow$ status) as well as a study of sensitivity about the change of the drift from a persistent direction to the opposite one (jibing) relative to downwind. This change will result in a sign change on the crosswind component. The jibing is set in the model as a frequency fixed on all the simulation time. Such information is very important: if the object doesn't jibe, the initial probability distribution could rapidly split in two equal probability distant areas, according to the initial uncertainty about the tack relative to downwind. On the contrary, the more frequent is the jibing, the more central is the distribution (Allen et al., 2010).

We check a jibing frequency from 1% to 8% for each tabled position.

The second set of experiments is performed after choosing the best solution from the previous study: in the regression line used to calculate the downwind and crosswind $leeway$ components, we check different coefficients of the time-invariant Gaussian perturbation (ϵ_n) which Breivik and Allen (2008) introduced to include the variance increasing with wind speed.

Finally we carry out the third set of experiments: here the solutions are calculated using the $almost$ deterministic approach. The human body geometry is assimilated to a cylinder with a ratio height/width between 4 and 7, according to Hoerner (1965); then the projected frontal area, that is predominantly responsable for the drag, is calculated. Due to air in the lungs we suppose that the body is submerged in standing position up to thorax and then we calculate both the submerged and emerged part. To include the error about the calculation of the real surface exposed to the flow, we introduce two different perturbations: a vertical random oscillation between the thorax and the neck and a random rotation around the vertical axis; at the same time we assume a nonsignificant Stokes drift. Many experiments are performed to find the critic Reynolds number which marks the transition from laminar to turbulent boundary layer. Each critic values between 120000 and 170000 is coupled with all drag coefficients between 0.98 and 1.12 (the latter estimated according to Zdravkovich (1997) curves) resulting in different runs. At last we find the critic Reynolds number and the drag coefficient corresponding to the solution where the distance between the seeded particles subsets and the retrieval point/time is the shortest.

To check the reliability of the $almost$ deterministic approach we run the model in a different geographycal area, using a target $similar$ to a person and referring to the critic Reynolds number vs drag coefficient found in the last experiment. The data, provided by the Italian Coast Guard, were colletcted during a SAR training: on November 13^{th} 2013 at UTC 8:30pm a dummy was seeded in the Sicily Channel and it was retrieved 13 hours later.

The geometrically scaled target and the statistic of the new forcings are included in the model; we estimate on the forcings a standard deviation 0.09 $m \cdot s^{-1}$ in current east component and 0.11 $m \cdot s^{-1}$ in the north one, while it is 4.07 $m \cdot s^{-1}$ in wind east component and 4.25 $m \cdot s^{-1}$ in the north one.

The data about latter experiment are shown in the Tab. 3 and 4.

3 Results

In this section the main results of each set of experiments are shown. The first set of experiments is about the configuration of the target and the effects of the corresponding jibing. Here the $unknown$ status, which has the highest error variance in the statistical calculation of the $leeway$, gives the best results; changing the jibing values the results don't change significatively. This is why we opt for the LEEWAY standard value 4%. The final map is shown in Fig. 2 where at the retrieval time the target is outside the particles cloud. The distance between the mass center of each seeding group and the retrieval point/time is shown in Fig. 3: we verify that the 3^{rd} group, seeded between the 9:30am and 10:00am, is the closest to the target, with a distance which oscillates around the value of 9 km; the smallest absolute distance (about 2 km) is reached 31.5 hours later relative to the retrieval time by the 4^{rd} group one, seeded between the 10:00am and 10:30am.

The second set of experiments studies the influence of the perturbation coefficients on the results. These coefficients have been added in the regression line used to calculate the $leeway$, to include the variance increasing with the wind speed. In our experiments we verify that the spread is such that the particles final cloud includes the target at retrieval time (Fig. 4) when the slope is a_n=a+ϵ_n/5 and the offset is b_n=b+2 $\cdot\epsilon_n$, i.e. the perturbation coefficients are 4 times greater than the ones proposed in Breivik and Allen (2008) . The 3^{rd} group is again the nearest to the retrieval point and the relative distance oscillates around the value of 5.5 km (Fig. 5); such group has the absolute smallest distance (about 4.3 km) 5 hours later relative to the retrieval time. As a result the uncertainty about the time of the accident is reduced and the distance between the mass center of the favoured seeded group and the retrieval point is almost halved but the dispersion is now very higher.

To reduce the dispersion and to give a greater weight to the advection, a different option about the perturbation coefficients is checked: if wind velocity is lower than 10 $m \cdot s^{-1}$ we increase only the offset perturbation coefficient whereas for wind velocity greater that 10 $m \cdot s^{-1}$ we increase only the slope one, according to different weight of the offset/slope of the regression line at lower/higher wind speeds. Now the particles cloud includes the target at the rescue time and the dispersion of the particles is reduced (Fig. 6) but the distance between the mass center of the 3^{rd} group and the retrieval point/time is very similar to that one in the first experiment, resulting be about 8.9 km (Fig. 7). As in the first experiment, the 4^{rd} seeded group has again the smallest absolute distance (about 2.8 km) 31.5 hours later relative to the retrieval time.

The previous experiments pointed out the different performances of the model when the real statistic on forcings and the statistical regression line to calculate the $leeway$ velocity are used. Not only the heteroscedasticity of the experimental dataset compiled by Allen and Plourde (1999) needs to be correctly accounted for to optimize the model performances, but we also need to choose the best perturbation coefficients to use in the regression line. We don't know them in advance and we only can say that they should be such that the dispersion doesn't swamp the advection role and at the same time it should induce to maximize the POC.

The third set of experiments consists in simulating the PIW drift by means of the $almost$ deterministic law. After checking the projected frontal area by means of the allometric parameters for a "standard human body" according to Herman (2006), we choose a height/width ratio equal to 4.44. The final critic Reynolds number range is estimated between 165000 and 168000. The Reynolds numbers height based are always between O(10^4) and O(10^5); due to these values and to roughness role on

the boundary layer modifications (Yeo and Jones, 2011) we conclude that the PIW boundary layer in our experiment is often laminar with transition to turbulence prevalently precritic. That means that the drag crisis never occurs, the boundary layer never separates and the drag coefficient in the turbulent boundary layer is constant for a large Reynolds numbers range. In our experiments the drag coefficient corresponding to the best results is 1.12. All the parameters to solve the forces balance equation are in the Tab. 2.

The results now show that at retrieval time the cloud includes the target (Fig. 8) and at same time the dispersion of the particles looks low and qualitatively comparable with that one in Fig. 6 where the $leeway$ perturbation coefficients have been setted separately on the slope or on the offset of the regression line according to wind velocity. The absolute distance of 3^{rd} group of particles from the rescue point is minimum (Fig. 9) and is about 1.3 km.

In the figure 10, where the snapshots of figure 9 are showed without the probability map, it is visible that the particles move according to surface hydrodynamic; some mesoscale and sub-mesoscale cyclonic and anticyclonic structures are visible, according to complex circulation of the area as described in Pascual et al. (2013), Rinaldi et al. (2010), Iacono et al. (2013), Astraldi and Gasparini (1994). In particular, the area where the particles are seeded is characterized by three principal surface structures: two cyclonic gyres (named "A" and "C"), separated by an anticyclonic gyre (named "B"). The cyclones "A",located in the area $9.85° - 11.3°$E, $39.3° - 40.25°$N, and "C", located in the area $10° - 10.75°$E, $40.5° - 41.1°$N are persistent during the period of the simulation and show circulation features according to summer time ones as described in Rinaldi et al. (2010) and Marullo et al. (1994). The most of particles are seeded along the western brunch of the gyre "A" while the smallest amount is seeded between the cyclonic gyre "C" and the antyciclonic gyre "B". On the time the particles set is separated in two subsets: the gyre "A" track the larger subset westwards near the Sardinia coast while the variability of the current between the gyres "C" and "B" tracks the remaining particles to the open sea. Due to this analysis we conclude that the persistent summer gyre "A" is responsable for the motion of PIW in our experiment and we think that in all probability the person fell in water north of the retrieved point.

We checked our approach in a different area (Sicily Channel), using experimental data (Tab. 3) and scaling geometrically our target (Tab. 4). The results show that the target is inside the particles cloud, which minimum distance, estimated about in 5.8 km, is reached at the rescue time (Fig. 11). The target is located on the external border of the cloud (Fig. 12), then the POC is from medium to low value. The figure 13 shows that the particles cloud is seeded on the external part of an anticyclonic vortex, in an area where the current flowing along the southern Calabria coastline interacts with the current coming from the Messina Strait, separating the Sicily Island from the Italian Peninsula. It is a narrow passage where the Tyrrhenian and Ionian Sea sub-basins are interconnected: the interaction between its bathymetry and topography and the strong currents induces the generation of inertial eddies and strong horizontal current shears, generally located at along both Sicily and Calabria main capes (Cucco et al., 2016). Although the Mediterranean Sea is characeterized by very small tidal displacements which don't influence significatively the circulation (Sannino et al., 2015), in the Messina Strait large gradients of tidal displacement are registered because the semidiurnal tides in the Tyrrhenian and Ionian Sea are approximately in phase opposition. The tides then in the Messina Strait are the principal forcing of the circulation which develops mainly along the main axis of the channel; in particular, during the flood the flow is northward whereas during the ebb the flow is southward (Cucco et al., 2016).

Our experiment was performed during the ebb phase; the dummy was seeded in an area where northern border of the anticyclonic vortex, located in the area $15.3° - 16.3°$E, $37.2° - 37.65°$N, mixes with both the surface flow carrying the Ionian waters from the southern Calabria coastline to Sicily eastern coastline and part of the current coming from Messina Strait. The area is therefore characterized by an high turbulence which plays an important role on the particles dispersion.

In general, the figure 10 such as the figure 13 underline the importance to have an efficient operational ocean prediction system for the SAR activities not only because it is the forcing of the dispersion lagrangian model, but also because it gives many informations useful to analyze the particles cloud final evolution. In particular, in the figure 13, it seems that approximation on the POC calculation is greater than that one estimated in the Sardinia experiment but we think that it can be improved if the set of particles is clustered according not only to seeding time but also splitting the cloud in subsets as much as are the hydrodynamic structures; in this way each subset will have an own POC which could be high even if the it includes a small number of particles. We are currently working to this hypothesis.

4 Conclusions

We have presented the results of numerical experiments performed to estimate the Probability of Containment (POC) of Person in Water (PIW). We have referred to a real event occurred in the western Thyrrenian sea. The LEEWAY model, nested with the sub-regional hydrodynamic model TSCRM has been used. The real statistic of the forcings on the observation period was accounted for and the Last Known Position has been based on the trajectory of the ferry during 3.5 hours, recorded by the Automatic Information System; to reproduce the event a set of 1000 particles seeded in 8 time step has been used.

The objective of the work has been to validate an $almost$ deterministic law to calculate the $leeway$, based on the boundary layer theory; these results have been compared with those obtained estimating the $leeway$ by means of the standard statistical approach. The latter has produced the best results when the perturbation coefficients in the regression line have been changed separately on the offset or on the slope of the regression line according to wind velocity.

To calculate the $leeway$ in the $almost$ deterministic approach the PIW has been cylynder-shaped with a height/width ratio equal to 4.44; the critic Reynolds number has been found in the range between 165000 and 168000 and the drag coefficients have been estimated equal to 1.12. Now the results have showed that at the retrieved time the particles cloud includes the target and the 3^{rd} subset of particles is representative of the event then we also can estimate the time of the accident with good approsimation. The results estimated by means of the standard statistical approach are similar but with the new approach the distance of the mass center of the favoured subset of particles is strongly reduced 6.5 times, resulting of $1.3km$. The tests in Sicily Channel using a similar target have confirmed the reliability of the method.

A second important result is that the particles distribution in both experiments is coherent with the hydrodynamic structures, highlighting the importance to have an efficient operational ocean prediction system for the SAR activity: the hydrodynamic field is required not only because it forces the lagrangian model but also because it allows to read the final results in a more full way. We think infact that the results about the POC can be improved splitting the set of particles in subsets as much as are hydrodynamic structures, so that each subset can significatively contribute with the own POC; it corresponds to consider

time-evolving probability density functions of the location of the search object as much as are the hydrodynamic structures. At last, the Stokes drift will have also to be included.

The results here obtained encourage to explore other different target categories. We believe that on the long time it will allow to overcame the limitations connected with the standard approach based on the tabled statistical parameters, providing leeway-drift formulas for practical use based on appropriate Reynolds critic numbers and drag coefficients for specific targets. This idea is supported by the realistic option to execute tests in naval tank, simulating different meteomarine conditions, scaling opportunely specific targets and then overcoming the costs and difficulties to acquire field data.

Acknowledgements. We would like to thank to C.te Sirio Faé of Italian Coast Guard for providing the data about our experiments and for supporting in the interpretation of the IAMSAR Manual. Thanks also to collegues of the CNR-INSEAN: Massimo Miozzi for his constructive comments during the work and Paola Carratú for her special contribution.

This study was supported by the Italian Project PON-TESSA (PON01-02823) and by RITMARE (Ricerca ITaliana per il MARE) Flagship Project of Italy (PNR 2011-2013,approved by CIPE with adjudication 2/2011 on 23/03/2011), funded by the Ministry for Education, University and Research of Italy - MIUR.

References

Abascal, A. J., Castanedo, S., Medina, R., Losada, I. J., and Alvarez-Fanjul, E.: Application of HF radar currents to oil spill modelling, Marine Pollution Bulletin, 58, 238–248, 2009b.

Abascal, A. J., Castanedo, S., Fernández, V., and R., R. M.: Backtracking drifting objects using surface currents from high-frequency (HF) radar technology, Ocean Dynamics, 62, 1073–1089, 2012.

Allen, A., Roth, J. C., Maisondieu, C., Breivik, Ø., and Forest, B.: Drift of Common Search and Rescue Field Determination of the Leeway of Drifting Objects, Tech. rep., Norwegian Meteorological Institute, Met.No, 2010.

Allen, A. A.: Leeway Divergence Report, Tech. rep., US Coast Guard Research and Development Center, 2082 Shennecossett Road, Groton, CT, USA, 2005.

Allen, A. A. and Plourde, J.: Review of Leeway: Field Experiments and Implementation, Tech. rep., US Coast Guard Research and Development Center, 2082 Shennecossett Road, Groton, CT, USA, 1999.

Astraldi, M. and Gasparini, G. P.: The Seasonal Characteristics of the Circulation in the Tyrrhenian Sea, Coastal and Estuarine Studies, 46, 115–134, 1994.

Barrick, D., Fernandez, V., Ferrer, M. I., Whelan, C., and Breivik, Ø.: A shor-term predictive system for surface currents from a rapidly deployed coastal HF radar network, Ocean Dynamics, 62, 725–740, doi:10.1007/s10 236–012–0521–0, 2012.

Barrick, D. E., Evans, M. W., and Weber, B. L.: Ocean surface currents mapped by radar, Science, 198, 138–144, 1977.

Bell, M. J., Lefebvre, M., Traon, P.-Y. L., Smith, N., and Wilmer-Becker, K.: GODAE: The Global Ocean Data Assimilation Experiment Forecasting., Oceanography, 22, 14–21, 2009.

Bell, M. J., Schiller, A., Traon, P. Y. L., Smith, N. R., Dombrowsky, E., and Wilmer-Becker., K.: An introduction to GODAE OceanView, Journal of Operational Oceanography, 8, 2–11, 2015.

Bellomo, L., Griffa, A., Cosoli, S., Falco, P., Gerin, R., Iermano, I., Kalampokis, A., Kokkini, Z., Lana, A., Magaldi, M., Mamoutos, I., Mantovani, C., Marmain, J., Potiris, E., Sayol, J., Barbin, Y., Berta, M., Borghini, M., Bussani, A., Corgnati, L., Dagneaux, Q., Gaggelli, J., Guterman, P., Mallarino, D., Mazzoldi, A., Molcard, A., Orfila, A., Poulain, P.-M., Quentin, C., Tintoré, J., Uttieri, M., Vetrano, A., Zambianchi, E., and Zervakis, V.: Toward an integrated HF radar network in the Mediterranean Sea to improve search and rescue and oil spill response: the TOSCA project experience, Journal of Operational Oceanography, doi: 10.1080/1755876X.2015.1087184 http://dx.doi.org/10.1080/1755876X.2015.1087184, 2015.

Berta, M., Bellomo, L., Magaldi, M. G., Griffa, A., Molcard, A., J., J. M., Borghini, M., and Taillandier, V.: Estimating Lagrangian transport blending drifters with HF radar data and models: results from the TOSCA experiment in the Ligurian Current (North Western Mediterranean Sea), Progress in Oceanopgraphy, 128, 15–29, 2014.

Blumberg, A. F. and Mellor, G.: A description of a threedimensional coastal ocean circulation model,, American Geophysical Union, 208, 1–16, 1987.

Brassington, G., Pugh, T., , Spillman, C., Schulz, E., Beggs, H., Schiller, A., and Oke, P.: BLUElink: Development of operational oceanography and servicing in Australia., Journal of Research and Practice in Information Technology, 39, 151–164, 2007.

Breivik, Ø. and Allen, A.: An operational search and rescue model for the Norwegian Sea and the North Sea, Journal of Marine System, 69, 99–113, 2008.

Breivik, Ø., Allen, A., Maisondieu, C., Roth, J.-C., and Forest, B.: The Leeway of shipping containers at different immersion levels., Ocean Dynamics, 62, 741–752, 2012.

Breivik, Ø., Allen, A. A., Maisondieu, C., and Olagnon, M.: Advances in Search and Rescue at Sea, Ocean Dynamics, 63, 83–88, 2013.

Carrara, P., Corgnati, L., Cosoli, S., Forneris, V., Griffa, A., and et al.: The RITMARE coastal radar network and applications to monitor marine transport infrastructures, in: EGU General Assembly, vol. 16, Wien, Austria, 2014.

Cianelli, D., Iermano, I., Mozzillo, P., Uttieri, M., Zambardino, G., Buonocore, B., Falco, P., and Zambianchi, E.: Inshore/offshore water exchange in the Gulf of Naples, Journal of Marine Systems, 145, 37–52, 2015.

Cucco, A., Quattrocchi, G., Olita, A., Fazioli, L., Ribotti, A., Sinerchia, M., Tedesco, C., and Sorgente, R.: Hydrodynamic modeling of coastal seas: the role of tidal dynamics in the Messina Strait , Western Mediterranean Sea, Natural Hazards Earth System Science Discussion, doi:10.5194/nhess-2016-75, 2016.

Davidson, F., Allen, A., Brassington, G., Breivik, Ø., Daniel, P., Kamachi, M., Sato, S., King, B., Lefevre, F., Sutton, M., and Kaneko, H.: Applications of GODAE ocean current forecasts to search and rescue and ship routing, Oceanography, 22, 176–181, 2009.

Fazioli, L., Olita, A., Cucco, A., Tedesco, C., Ribotti, A., and Sorgente, R.: Impact of different initialization methods on the quality of the sea surface temperature forecasts for the Sicily strait area, Subb. to Journal Operational Oceanography, 2015.

Hackett, B., Breivik, Ø., and Wettre, C.: Forecasting the drift of objects and substances in the oceans, in: Ocean Weather Forecasting, edited by Chessignet, E. and Verron, J., pp. 507–523, Springer, 2006.

Herman, I. P.: Physics of the Human Body, Biological and Medical Physics, Biomedical Engineering, 2006.

Hoerner, S. F.: Fluid-Dynamic Drag, theoretical, Experimental and Statistical Information, Practical Information on Aerodynamic Drag and Hydrodynamic Resistance, 64-19666, 1965.

Iacono, R., Napolitano, E., Marullo, S., and Artale, V.: Seasonal variability of the Tyrrhenian Sea surface geostrophic circulation as assessed by altimeter data, Journal of Physical Oceanography, 43, 1710–1732, 2013.

Koch, S. and McQueen, J.: A survey of nested grid techniques and their potential for use within the MASS weather prediction mode, NASA Techical Memorandum, 87, 1–25, 1987.

Marullo, S., Santoleri, R., and Bignami, F.: The surface characteristics of the Tyrrhenian Sea: Historical satellite data analysis, Coastal and Estuarine Studies, 46, 135–154, 1994.

Mellor, G.: An equation of state for numerical models of oceans and estuaries, J. Atmos. Oceanic Tech., 8, 609–611, 1991.

Mellor, G. and Yamada, T.: Development of a turbulence closure model for geophysical fluid problems, Rev. Geophys., 20, 851–875, 1982.

Oddo, P., Adani, M., Pinardi, N., Fratianni, C., Tonani, M., and Pettenuzzo, D.: A Nested Atlantic-Mediterranean Sea General Circulation Model for Operational Forecasting., Ocean Science, 5, 461–473, 2009.

Paduan, J. D. and Rosenfeld, L. K.: Remotely sensed surface currents in Monterey Bay from shore-based HF radar (CODAR), Journal of Geophysical Research, 101, 20 669–20 686, 1996.

Pascual, A., Bouffard, J., S. Ruiz, B. B. N., Vidal-Vijande, E., Escudier, R., Sayol, J. M., and Orfila, A.: Recent improvements in mesoscale characterization of the western Mediterranean Sea: synergy between satellite altimetry and other observational approaches, Scientia Marina, 77, 19–36, 2013.

Pinardi, N., Allen, I., Demirov, E., Mey, P. D., Korres, G., Lascaratos, A., Traon, P. Y. L., Maillard, C., Manzella, G., and Tziavos, C.: The Mediterranean ocean Forecasting System: first phase of implementation (1998-2001)., Annales Geophysicae, 21, 3–20, 2003.

Quentin, C., Barbin, Y., Bellomo, L., Forget, P., Gagelli, J., and et al.: HF radar in French Mediterranean Sea: an element of MOOSE Mediterranean Ocean Observing System on Environment, in: Ocean and Coastal Observation: Sensors ans observing systems, numerical models and information, pp. 25–30, Nice, France, 2013.

Richardson, P. L.: Drifting in the wind: leeway error in shipdrift data, Deep Sea Research I, 44, 1807–1903, 1997.

Rinaldi, E., Nardelli, B. B., Zambianchi, E., Santoleri, R., and Polin, P. M.: Lagrangian and Eulerian observation of the surface circulation in the Tyrrhenian Sea, Journal of Geophysical Research, 115, 1–13, 2010.

Sannino, G., Carillo, A., Pisacane, G., and Naranjo, C.: On the relevance of tidal forcing in modelling the Mediterranean thermohaline circulation, Progress in Oceanography, 134, 304–329, 2015.

Smagorinsky, J.: Some historical remarks on the use of nonlinear viscosities, in: Large eddy simulations of complex engineering and geophysical flows, Cambrige Univ. Press, pp. 1–34, 1993.

Sorgente, R., Drago, A., and Ribotti, A.: Seasonal variability in the Central Mediterranean Sea circulation,, Ocean Science, 21, 299–322, 2003.

Sorgente, R., Olita, A. ., Oddo, P., Fazioli, L., and Ribotti, A.: Numerical simulation and decomposition of kinetic energy in the Central Mediterranean: insight on mesoscale circulation and energy conversion, Ocean Science, 7, 503–519, 2011.

Tonani, M., Pinardi, N., Dobricic, S., Pujol, I., and Fratianni., C.: A High Resolution Free Surface Model on the Mediterranean Sea, Ocean Science, 4, 1–14, 2008.

Tonani, M., Balmased, M., Bertino, L., Blockley, E., Brassington, G., Davidson, F., Driller, Y., Hogan, P., Kuragano, T., Lee, T., Mehra, A., Paranathara, F., Tanajura, C., and Wang, H.: Status and future of global and regional ocean prediction systems, Journal of Operational Oceanography, 8, 201–220, 2015.

Ullman, D., O'Donnell, J., Edwards, C., Fake, T., Morschauser, D., Sprague, M., Allen, A., and Krenzien, B.: Use of Coastal Ocean Dynamics Application Radar (CODAR) technology in U. S. Coast Guard search and rescue planning, Tech. rep., U.S. Coast Guard Research and Development Center, 2003.

Ullman, D. S., O'Donnell, J., Kohut, J., Fake, T., and Allen, A.: Trajectory prediction using HF radar surface currents: Monte Carlo simulations of prediction uncertainties, Journal of Geophysical Research, 111, C12 005, doi:10.1029/2006JC00 371, 2006.

Yeo, D. and Jones, N. P.: Computational Study on 3-D Aerodynamic Characteristics of Flow around a Yawed, Inclined, Circular Cylinder, Tech. rep., Newmark, 2011.

Zavatarelli, M., Pinardi, N., Kourafalou, V., and Maggiore, A.: Diagnostic and prognosticmodel studies of the Adriatic Sea general circulation: Seasonal variability, Journal Geophysical Research, 107, 1–20, 2002.

Zdravkovich, M.: Flow around circular cylindres, A comprehensive guide throug flow phenomena, Experiments, Applications, Mathematical Models and Computer Simulations, vol. 1, 1997.

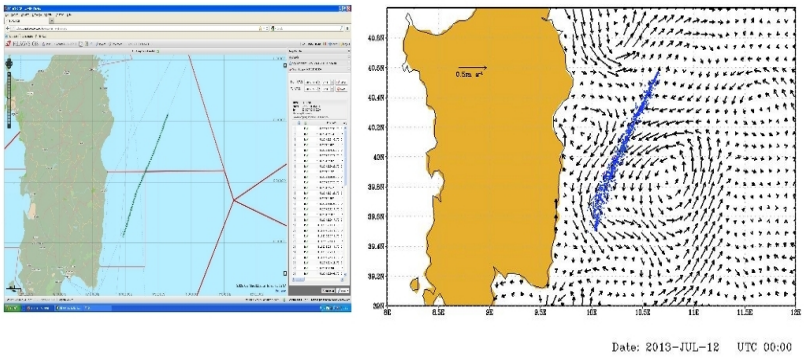

Figure 1. The Last Known Position, represented by the blue particles distribution at the alert time; it is based on the AIS system that gives the ferry position every 6 seconds (green line on the left of the picture). The coordinates of start and end point are defined in Tab. 1.

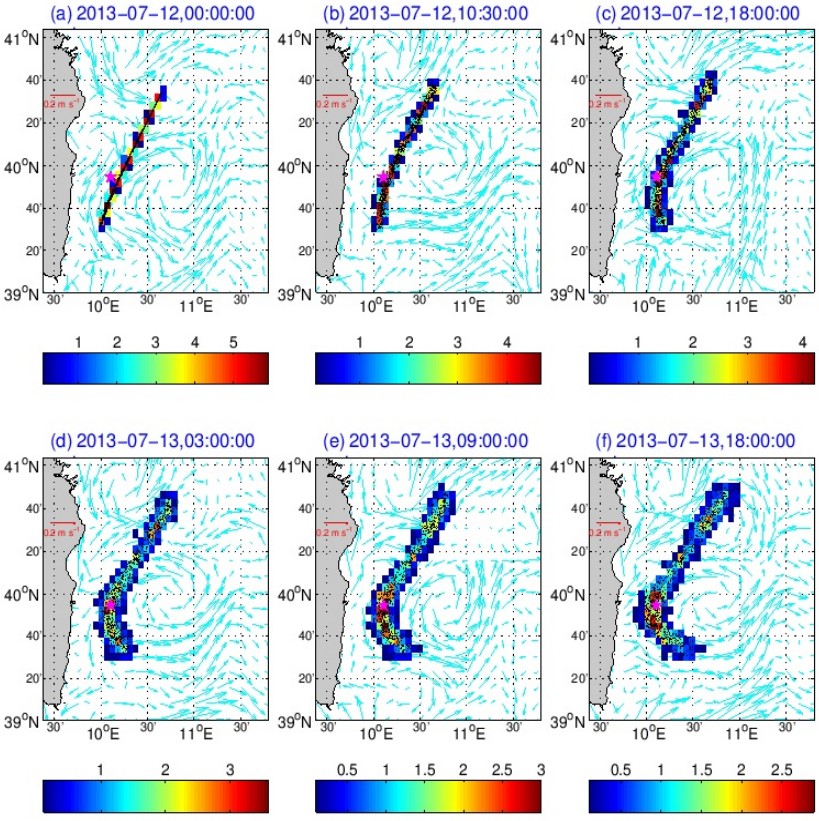

Figure 2. Particles cloud estimated by the LEEWAY model overlapped to the hydrodynamic field. Here the $leeway$ comes by statistical law as in Breivik and Allen (2008). The probability of containment (POC) also is computed and it varies from blue/minimum to red/maximum value in each grid box of 0.6x0.6°. At rescue time (subplot (b) in the panel), the target (magenta point) is outside the particles cloud; it will be included in the cloud only 7.5 hours late (subplot (c) in the panel).

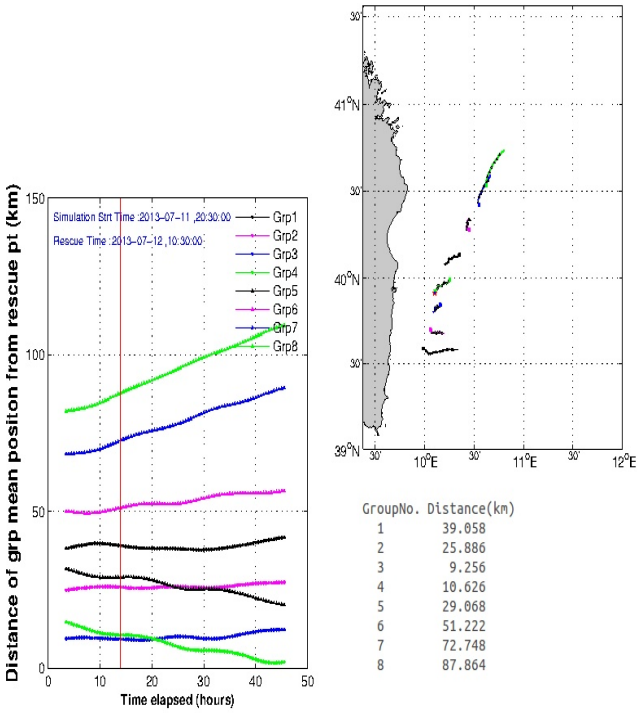

Figure 3. Distance of the mass center of each group seeded every 30 minutes from 8:30pm (Group 1) of the 11 july 2013 to next midnight (Group 8). The vertical red line marks the rescue time. Here the $leeway$ is calculated by means of the statistical law as in Breivik and Allen (2008). May be possible verify that the lower distances at the rescue time (values at right and low part of the panel) is reached by the mass center of the 3^{rd} subset of particles (seeded from 9:30pm to 10:00pm). The smallest distance is reached 31.5 hours later by the 4^{th} subset (seeded from 10:00pm to 10:30pm) and it is about 2 km. On the upper right side of the picture the trajectories of the each group mass center during all the simulation time (43 hours) are visible.

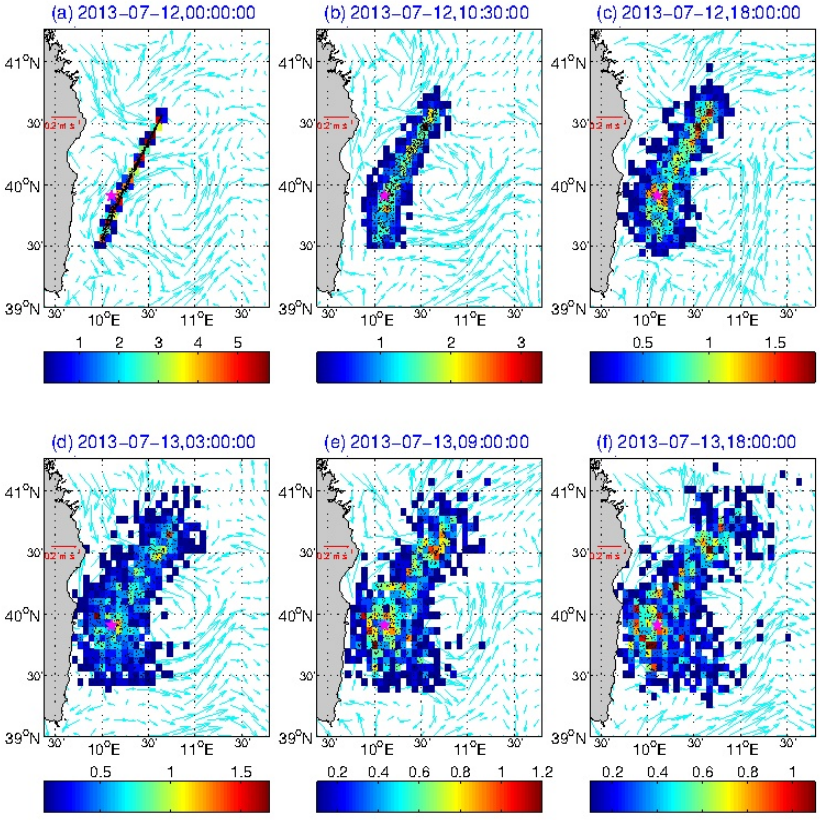

Figure 4. Here the perturbation coefficient is 4 time greater that one in Breivik and Allen (2008); in particular a common perturbation coefficient was setted at the same time either in slope and in the offset of the regression line. Now the particles cloud includes the target at the rescue time but the dispersion is much larger than that one in figure 2.

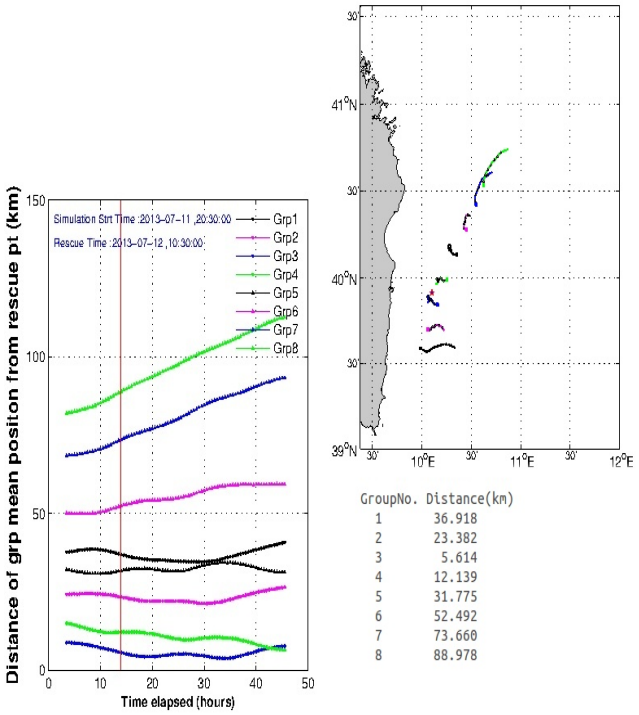

Figure 5. Distance of the mass center of each group seeded every 30 minutes from 8:30pm (Group 1) of the 11 july 2013 to next midnight (Group 8). The $leeway$ perturbation coefficient was setted at the same time on the offset and on the slope of the regression line as 4 times that ones corresponding to the results in figure 3. Now the mass center of 3^{rd} subset (seeded from 9:30pm to 10:00pm) has the smallest distance at the rescue time and it is about 5.6 km. The smallest absolute distance is about 4.3 km and it is reached 5 hours later by the same subset of particles. The trajectories of the each group mass center during all the simulation seem slowly changed respect to the precedent experiment.

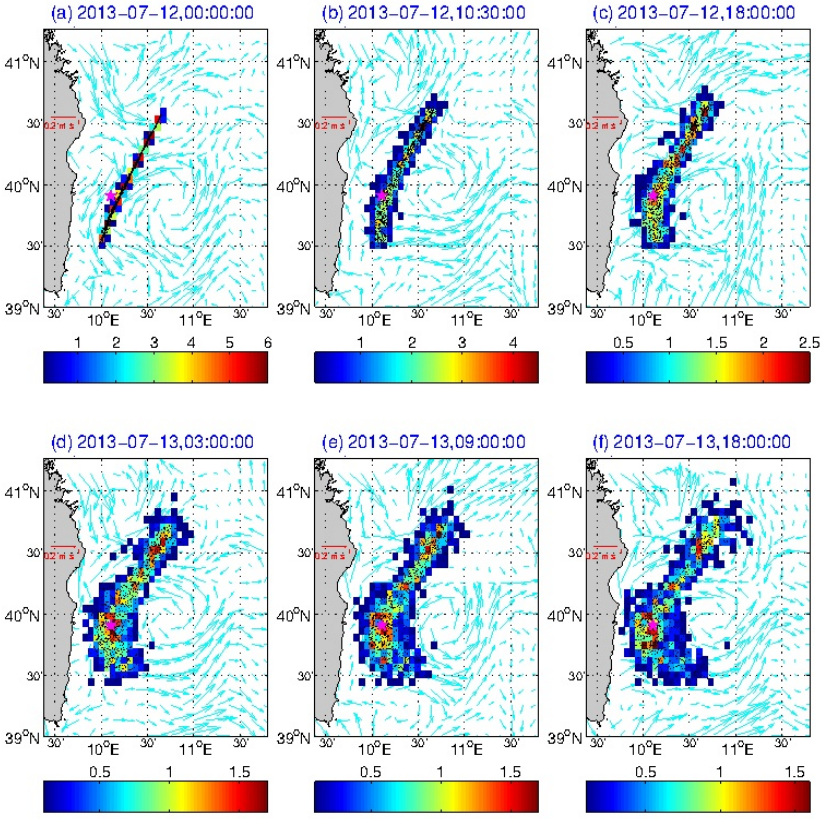

Figure 6. Here the common perturbation coefficient was setted separately on the offset or on the slope of the regression line according to the wind velocity: for wind velocity lower than 10 $m \cdot s^{-1}$ the $leeway$ perturbation coefficient is 4 time that one in Breivik and Allen (2008) only on the offset of the regression line while for wind velocity greater that 10 $m \cdot s^{-1}$ only that one of the slope was changed. The particles cloud includes the target at the rescue time (panel (b) in the figure) and the dispersion is reduced respect to that one in the precedent experiment.

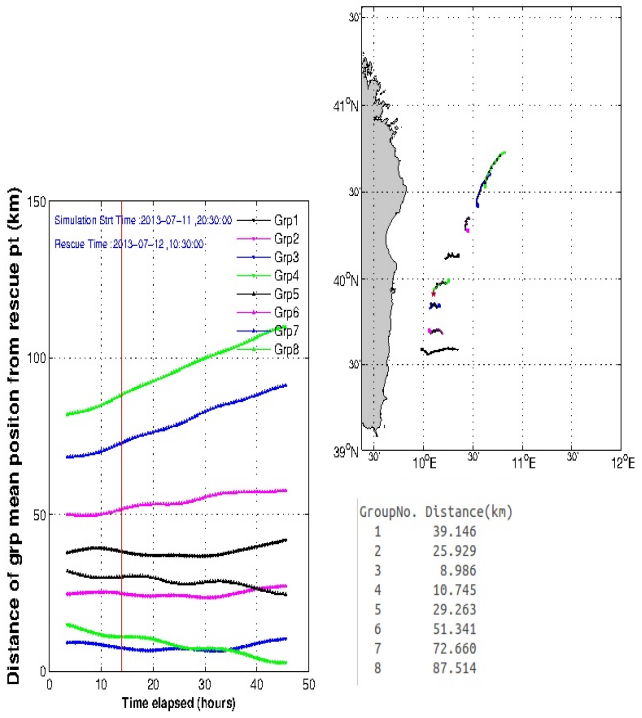

Figure 7. Distance of the mass center of each group seeded every 30 minutes from 8:30pm (Group 1) of the 11 july 2013 to next midnight (Group 8). The $leeway$ perturbation coefficient is setted separately on the offset or on the slope of the regression line according to wind velocity. Now the mass center of the 3^{rd} subset of particles (seeded from 9:30pm to 10:00pm) has the smallest distance at the rescue time: it is about 8.9 km and it is very similar to that one in the first experiment . The smallest absolute distance is about 2.8 km, estimated 31.5 hours later and it belongs to the mass center of the 4^{rd} group.

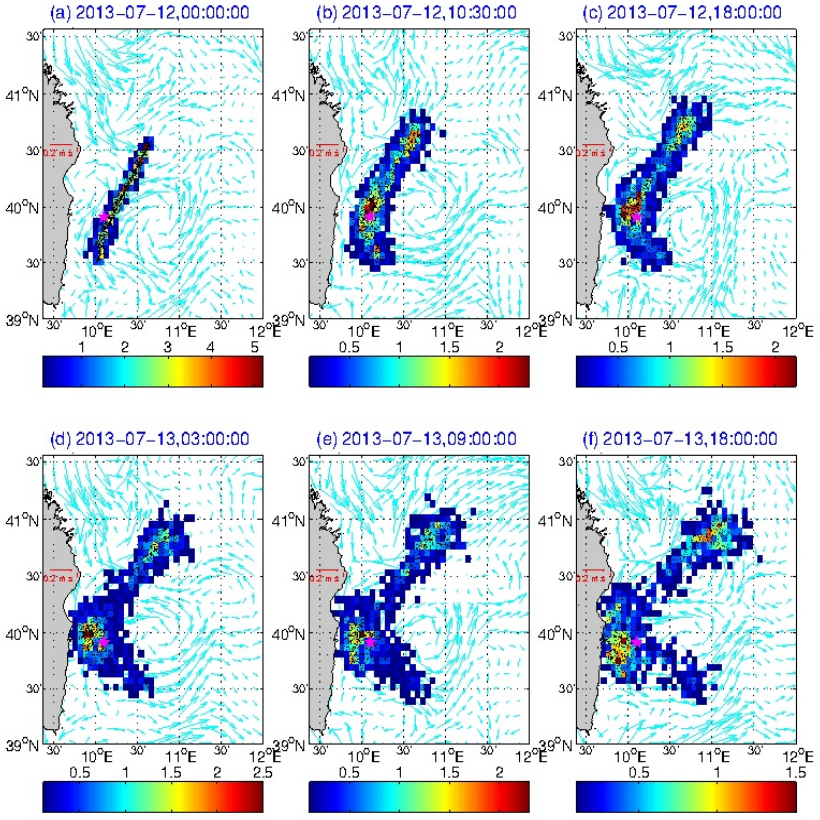

Figure 8. Particles cloud simulated by the model overlapped to the hydrodynamic structures. Here the $leeway$ is calculated by means of the forces balance equation. The cloud includes the target at the rescue time and the dispersion seems not to swamp the advection; in particular the particles cloud seems to separate on a large time according to hydrodynamic structures (subplot (e) and (f) in the panel).

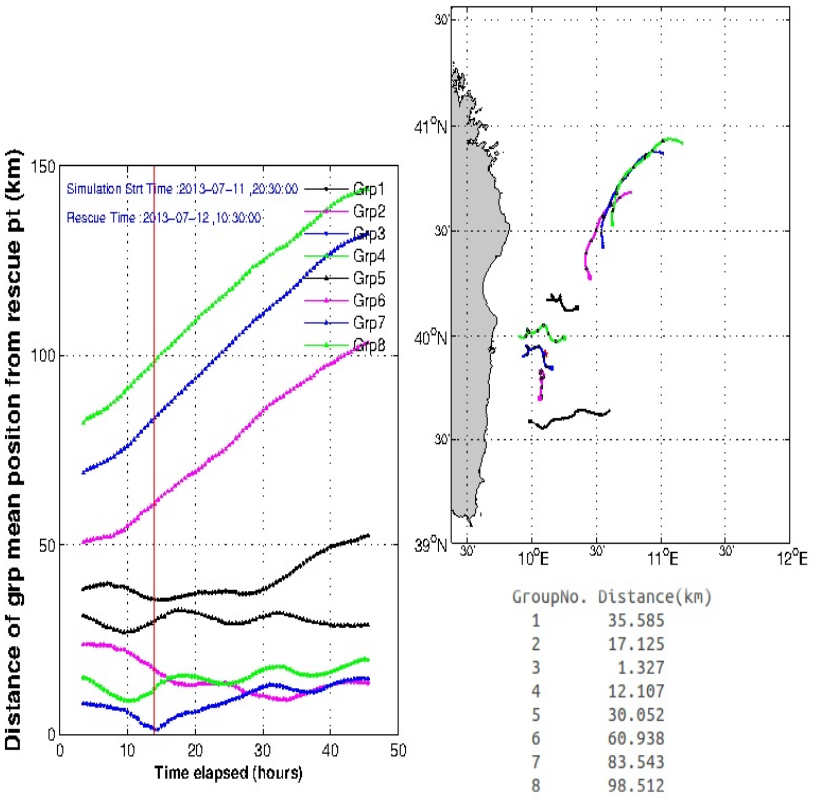

Figure 9. Distance of each seeded group mass center from the rescue time/space. The seeding was every 30 minutes from 8:30pm (Group 1) to midnight (Group 8). Here the $leeway$ is calculated by means of the forces balance equation. May be possible verify that now the solution is better than the previous ones: at the rescue time the 3^{rd} group (seeded from 09:30pm to 10:00pm) has the smallest absolute distance and it is about 1.3 km.

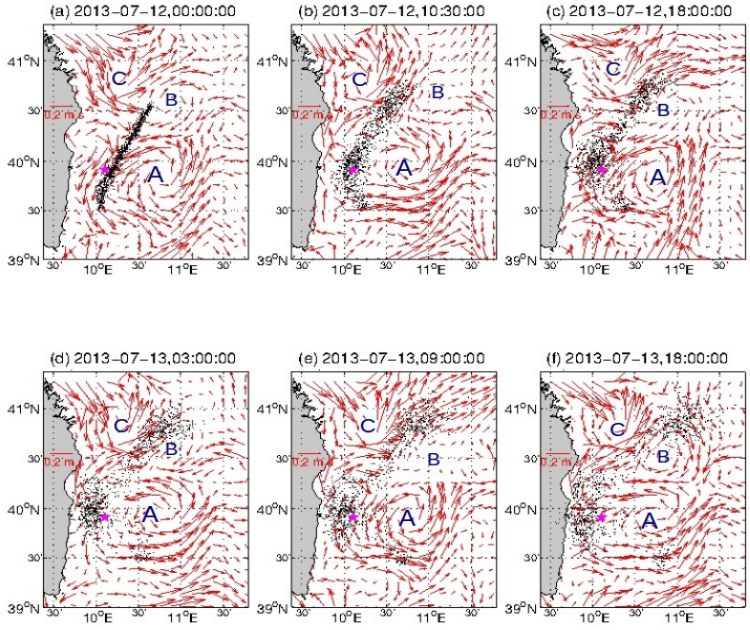

Figure 10. Particles dispersion in the Bonaria experiment, overlapped on the hydrodynamic field. Three principal surface structures are visible in the experiment are: two cyclonic gyres "A" and "C", separated by the anticyclonic gyre "B". The cyclones "A" and "C" are persistent during the period of the simulation. The most of particles are seeded along the western external part of the gyre "A" while the smallest amount is seeded between the cyclonic gyre "C" and the antyciclonic gyre "B". On the time the particles set is separated in two subsets: the gyre "A" track the larger subset westwards near the Sardinia coast whereas the variability of the current between the gyres "C" and "B" tracks the remaining particles to the open sea.

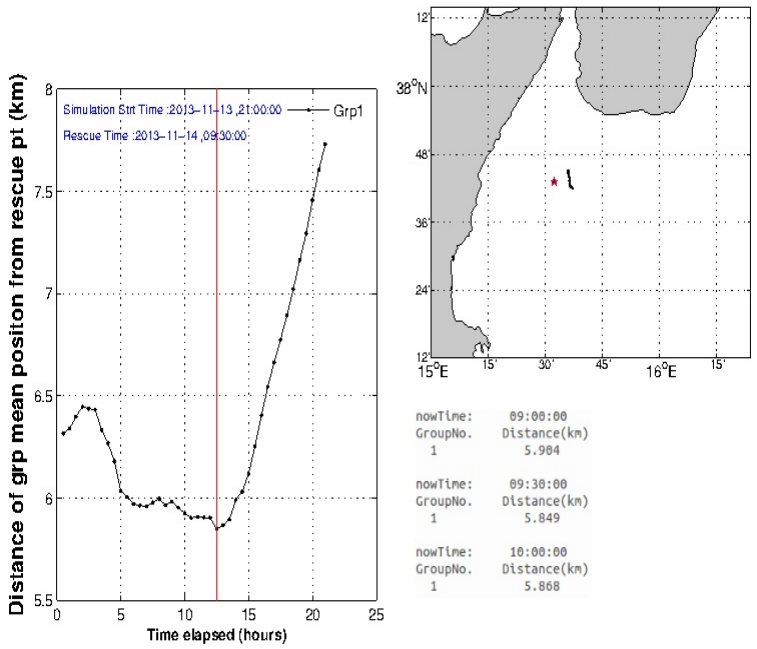

Figure 11. Distance of the mass center of the particles set seeded in a known time/point to simulate the trajectory of a dummy in the Sicily Channel. Again the $leeway$ is calculated by means of the forces balance equation. On the upper right side of the picture the trajectory of the mass center during all the period of the simulation (21 hours) is visible.

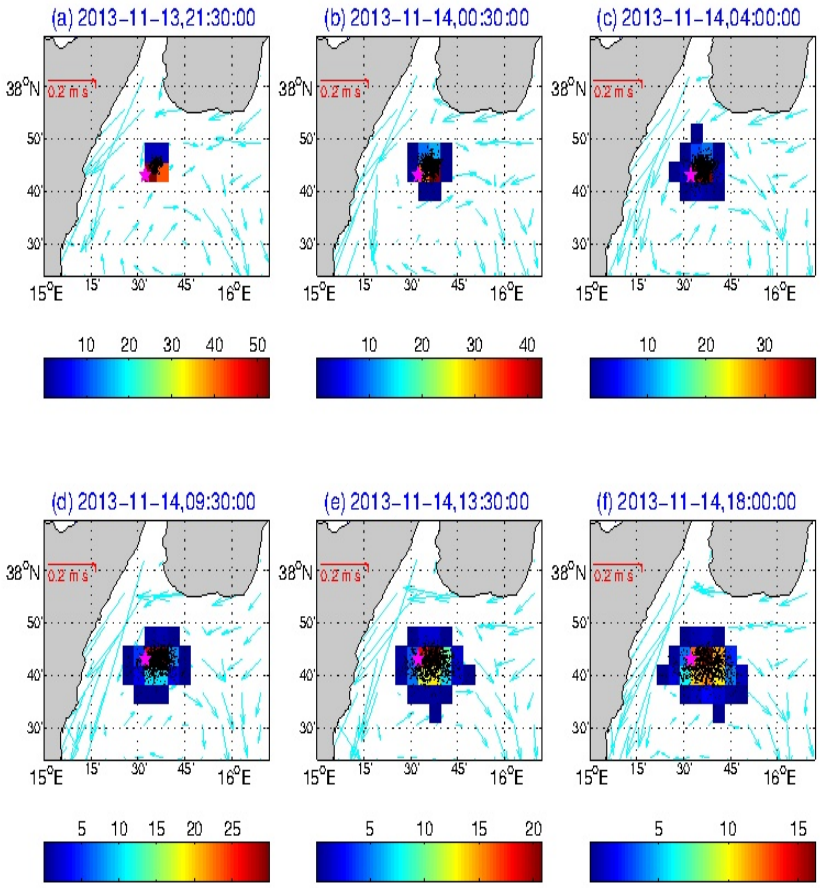

Figure 12. Particles cloud overlapped on the hydrodynamic field in the experiment executed in the Sicily Channel. In the panel (d) the configuration at the rescue time is visible. Far from the coast the current is prevalently easward but the particles subset influenced by the current near the coast well simulate the trajectory from the seeding point to the rescue point/time.

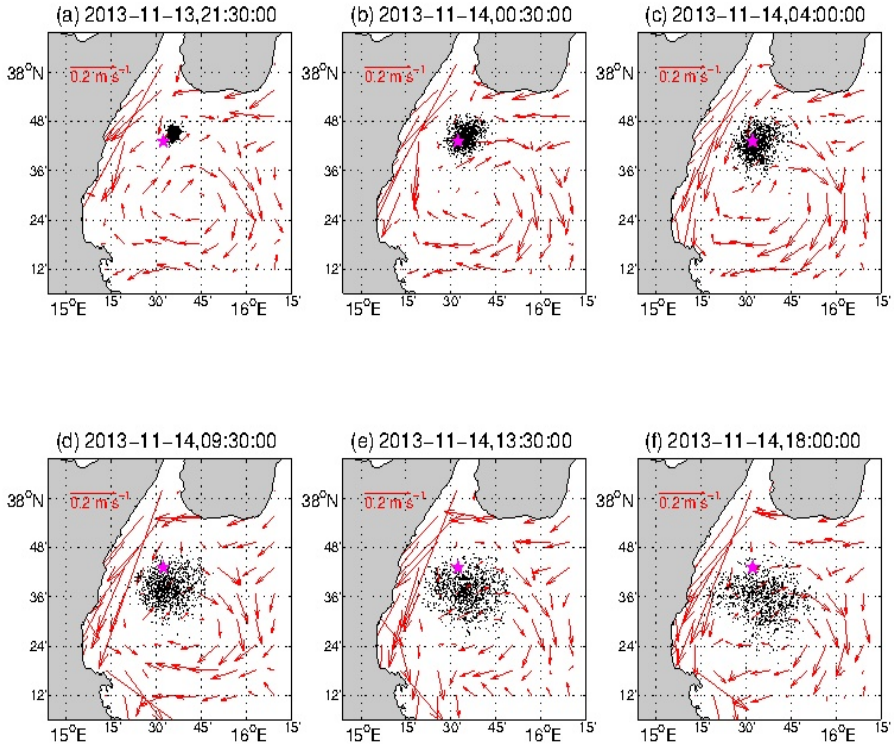

Figure 13. Particles dispersion in the Sicily Channel experiment, overlapped on the hydrodynamic field. The particles cloud is seeded on the external part of an anticyclonic vortex, where the current flowing along the southern Calabria coastline interacts with the strong current coming from the Messina Strait. The tides, principal forcings of the circulation which develops mainly along the main axis of the Strait, induce alternatively flood (northward flow) and ebb (southward flow): the dummy was seeded during the ebb phase. The particles are tracked according to the persistent anticyclonic vortex which east boundary is the strong current coming from the Messina Strait.

Table 1. Data inherent the incident

	ϕ	λ	Date (mm-dd-yyyy)	Time (UTC)
Start Point	$39^\circ\ 33.16'$N	$009^\circ\ 57.99'$E	07-11-2013	08:30 pm
End point	$40^\circ\ 34.04'$N	$010^\circ\ 38.99'$E	07-12-2013	00:00
Recovered point	$39^\circ\ 54.71'$N	$010^\circ\ 06.29'$E	07-12-2013	10:30 am

Table 2. Parameters used to solve the forces balance equation about the Person In Water

Water Density (kg/m^3)	1027.0
Water cinematic viscosity (m^2/sec)	$0.974 \cdot 10^{-6}$
Air Density (kg/m3)	1.2
Air cinematic viscosity (m^2/sec) at 20^oC and 1 atm	$1.41 \cdot 10^{-5}$
Human body Density (kg/m^3)	985.0
Standard Human Body weight (kg)	70
Standard Human Body height (m)	1.7
Critic Reynolds Number range	165000-168000
Water/Air Drag coefficient	1.12

Table 3. Data about the second experiment. A dummy seeded in a known point and rescued after 12.5 hours

	ϕ	λ	Date (mm-dd-yyyy)	Time (UTC)
Start/End Point	$37^\circ\ 45.00'$N	$015^\circ\ 36.00'$E	11-13-2013	08:30 pm
Recovered point	$37^\circ\ 43.00'$N	$015^\circ\ 32.32'$E	11-14-2013	09:30 am

Table 4. Parameters to solve the force balance equation for the dummy in the Sicily Channel

Water Density (kg/m^3)	1027.0
Water cinematic viscosity (m^2/sec)	$1.1 \cdot 10^{-6}$
Air Density (kg/m^3)	1.2
Air cinematic viscosity (m^2/sec) at 10^oC and 1 atm	$1.5 \cdot 10^{-5}$
Dummy weight (kg)	50
Dummy height (m)	1.5